NUCLEAR ENGINEERING

**MASSACHUSETTS INSTITUTE
OF TECHNOLOGY**

BOILING HEAT TRANSFER FOR HIGH VELOCITY FLOW
OF HIGHLY SUBCOOLED WATER

B. M. Lekakh[1], M. S. Kazimi and J. E. Meyer

October 1998

MITNE-315

BOILING HEAT TRANSFER FOR HIGH VELOCITY FLOW
OF HIGHLY SUBCOOLED WATER

B. M. Lekakh[1], M. S. Kazimi and J. E. Meyer

October 1998

MITNE-315

[1] The present address of B.M. Lekakh is: Atomic Energy of Canada Ltd., SP2F4, 2251 Speakman Drive, Mississauga, Ontario, Canada L5K 1B2.

ABSTRACT

The mechanisms and limitations of heat transfer in flow boiling of highly subcooled water in a nonuniformly heated channel are examined from both an experimental and a conceptual standpoint. The heat flux is evaluated utilizing measured temperatures on the surface of a copper block heated on a single side, and cooled through water flow in a central channel. The experiments covered water flow in a 9.5 mm diameter channel with velocities up to 20 m/s. The water subcooling was over 100°C for pressures between 2 and 3 MPa. A new correlation is proposed for the subcooled boiling region. Limits on heat transfer by various mechanisms at high heat fluxes are established. The homogeneous nucleation limit (spontaneous nucleation limit) on the heat flux and the limit for subcooled film boiling are defined and correlations are developed for their estimation.

TABLE OF CONTENTS

NOMENCLATURE

	VARIABLES	UNITS
A	Area	m^2
Bo	Boiling Number, $q / (G H_{fg})$	
CHF	Critical Heat Flux	W/m^2
c_p	Specific Heat at Constant Pressure	$J/(kg\ K)$
D	Diameter	m
G	Mass Flux	$kg/(m^2\ s)$
E	Enhancement Ratio	
F	Correction Multiplier	
f	Darcy Friction Factor	
H_{fg}	Heat of Vaporization	J/kg
h	Heat Transfer Coefficient	$W/(m^2\ K)$
I	Power Supply Current	A
J	Spontaneous Nucleation Rate per Unit Volume	$s^{-1}\ m^{-3}$
k	Conductivity	$W/(m\ K)$
Nu	Nusselt Number, $h\ D / k$	
P	Pressure	Pa
Pe	Peclet Number, $G\ D\ c_{pf} / k_f$	
pf	Peaking Factor	
Pr	Prandtl Number, $\mu\ c_p / k$	
q	Heat Flux	W/m^2
Re	Reynolds Number, $G\ D / \mu$	
S	Suppression factor	
St	Stanton Number, $q / (Gc_{pf} (T_s - T_b))$	
T	Temperature	K or °C
THN	Temperature of Homogeneous (Spontaneous) Nucleation	K or °C
U	Voltage	V
V	Velocity	m/s

	GREEK SYMBOLS	UNITS
ΔT	Temperature Difference	K
ΔP	Pressure Drop	Pa
γ	Normalized Subcooled Boiling Location	
μ	Dynamic Viscosity	Pa s
σ	Surface Tension	N/m
ρ	Density	kg/m^3
ψ	Non-Dimensional Heat Flux Parameter	

	SUBSCRIPTS
b	Bulk
c	Convective Term
CHF	Critical Heat Flux
f	Fluid (or Liquid)
fb	Film Boiling
g	Gas (or Vapor)
h	Heated
in	Incident
inc	Incoming
l	Liquid
limit	Limit
nb	Nucleate Boiling Term
ov	Overheating
q	Heat Flux
s	Saturation
sp	Single Phase
THN	Temperature of Homogeneous (Spontaneous) Nucleation
v	Velocity
w	Wall
x	Axial

	ACRONYMS
CHF	Critical Heat Flux
HEATING7.2	3-D Heat Conduction Code
THN	Temperature of Homogeneous (Spontaneous) Nucleation

LIST OF FIGURES

I. INTRODUCTION

This paper is focused on the mechanisms and limitations of heat transfer in flow boiling of high velocity water at high subcooling. The results of this study should help designers establish cooling requirements for high heat flux components, such as high power density research reactors, plasma facing components of fusion tokamaks, and targets of some intense beam accelerators. High heat flux technology must be developed in order to assure the reliability of these components. The heat fluxes of interest here are in the range of 10-20 MW/m^2, an order of magnitude higher than the peak heat fluxes in Light Water Reactors (LWRs). In recent years, a few investigators have produced data relevant to the very high heat and mass fluxes, mostly in connection with fusion technology development, as is the present work.

In fusion devices, energy deposition on a single-side of a metallic block is transferred by conduction towards a coolant channel which results in an axially and circumferentially non-uniform heat flux at the channel wall. A promising candidate cooling system is based on the use of highly subcooled water (subcooling more than 100°C) flowing at very high velocities (more than 5 m/s). These conditions are quite different from those used to obtain the vast majority of existing correlations for single-phase convection and subcooled nucleate boiling.

The Petukhov single-phase liquid convection correlation described by Boyd and Meng [1] is usually highly reliable for local turbulent forced convection heat transfer with variable physical properties during heating and is defined as follows:

$$h_{sp} = \frac{(k_f / D)(f / 8)Pe}{K_1 + K_2(f / 8)^{1/2}(Pr^{2/3} - 1)} \left(\frac{\mu_b}{\mu_w} \right)^{0.11} \tag{1}$$

where properties are evaluated at bulk conditions (T$_b$) except for μ_w which is evaluated at T$_w$; K$_1$ is a function of the Darcy friction factor (f); and K$_2$ is a function of Pr:

K$_1$ = 1+3.4 f

K$_2$ = 11.7+1.8 Pr$^{-1/3}$

Numerous equations to calculate the values of subcooled nucleate boiling heat transfer coefficients have been proposed. Some of these give very low values of wall superheat. A good example is the Jens-Lottes equation, which may be written in the following form (P in MPa, q in MW/m^2) [2]:

$$q = (2.56 \cdot 10^{-6})(\exp(P/1.55))(T_w - T_s)^4 \qquad (2)$$

where, for a given wall temperature, this nucleate boiling heat removal is applied only if it predicts a wall heat flux higher than possible by single phase convection: i.e., $q > h_{sp} (T_w - T_b)$; otherwise equation (1) should be applied.

However, in some experiments for high heat fluxes the wall superheat values were found to be much higher. Yin [3] empirically derived an equation applicable under fusion reactor thermal-hydraulic conditions and for a small channel diameter of 3.6 mm:

$$\Delta T_s = 7.195 \, q \, \gamma^{1.82} \, P^{-0.072} \qquad (3)$$

where q is in MW/m^2, P is in MPa, and γ = length at location of subcooled boiling as a fraction of total channel length. Equation (3) gives very large values of wall superheat in comparison with Equation (2). A subcooled nucleate boiling heat transfer can also be computed using the extension to the Chen [4] correlation originally suggested by Butterworth [5]:

$$q_w = h_c (T_w - T_b) F + h_{nb} (T_w - T_s) S \qquad (4)$$

where:

h_c is the single phase convective heat transfer coefficient given by

$$= 0.023 \, Re^{0.8} \, Pr^{0.4} \, k_f \, / \, D \qquad (5)$$

and, h_{nb} is the nucleate boiling heat transfer coefficient calculated using the original Chen correlation [4]:

$$h_{nb} = 0.00122 \, k_f^{0.79} c_{pf}^{0.45} \rho_f^{0.49} (T_w - T_s)^{0.24} \frac{(P_w - P_s)^{0.75}}{\sigma^{0.5} \mu_f^{0.29} \rho_g^{0.24} H_{fg}^{0.24}} \qquad (6)$$

where P_w and P_s denote the saturation pressure at T_w and T_s respectively. F and S are special factors to represent enhancement of single phase flow and suppression of nucleation respectively.

Shah [7] proposed the following correlation for the highly subcooled region:

$$q_w = \psi \, \Delta T_s \, h_c \qquad (7)$$

where the boiling effects are taken to enhance the convective flow heat transfer coefficient through the factor Ψ given by:

$$\psi = 1 + 46 \, Bo^{0.5} \quad \text{if } Bo < 0.3 \, 10^{-4}, \text{ or}$$

$$\psi = 230 \, Bo^{0.5} \quad \text{if } Bo > 0.3 \, 10^{-4}$$

The Chen and Shah equations take into account the two physical processes which occur in the nucleate boiling region: single phase heat transfer and heat transfer by vapor bubble formation/collapse. Equation (2) treats only the heat transfer removal by vapor bubbles, because q is proportional to $(T_W - T_s)^4$. Yin's correlation (Equation (3)) shows that ΔT_s is proportional to q, indicating dominant single-phase removal, although it reflects some heat removal by vapor bubbles. For high velocity conditions, nucleate boiling is suppressed, and at very high heat flux values, wall temperatures may approach the value of the Temperature of Homogeneous (Spontaneous) Nucleation (THN) [8,9]. There is no flow velocity in equation (3), which makes it impossible to determine when nucleate boiling is suppressed. The correlations of Chen (Equation (4)) and Shah (Equation (7)) both take into account single phase and nucleate heat removal. However, only Chen's correlation accounts for suppression of nucleate boiling at high velocities.

Kinoshita et al [27] reported the subcooled boiling heat transfer rate from a tube of 6.0 mm diameter at an exit pressure of 0.6 MPa for water velocity in the range 2<V<9 m/s. They observed a significantly more gentle slope for the q - ΔT_s curve at 9 m/s than at lower velocities (2 to 5 m/s), which could be the result of boiling suppression at the higher velocity. However their wall superheat, while reaching 100 K, did not apparently reach the thermodynamic THN limit.

On the basis of the short discussion given above, it can be concluded that validation and improvement of subcooled nucleate flow boiling correlations are necessary for the high heat flux,

high velocity region, where nucleate boiling can be suppressed and the thermodynamic spontaneous nucleation limit can be reached producing critical heat flux (CHF) conditions at a lower power than expected.

Hechanova [11], Simon-Tov [18] and Celata et al. [23] provided good reviews of CHF data as related to high heat and mass flux conditions. These reviews show that, except for a few investigators, the data are usually outside the high mass flux, high subcooling region or are for small channels (d<5mm). Also, most CHF experiments were performed using channels with uniform heat fluxes. This paper presents results for asymmetrical energy deposition. This deposition is very important from a practical point of view since many of the high heat flux devices of interest have nonuniform heat deposition. Azimuthally nonuniform heating experiments were carried out by Nariai et al [24] and Gaspari [25]. The focus of these experiments was on CHF values. Gaspari observed that at similar exit subcooling, the local CHF values for uniform and non-uniform heating were similar, indicating the dominance of local phenomena in determining the CHF condition.

Physical descriptions in the literature of possible causes for critical heat flux occurrences in subcooled boiling include the following:

(a) Near-wall bubble crowding and vapor blanketing.

A bubble boundary layer accumulates at the heated wall and becomes so dense that it effectively prevents fresh subcooled liquid from reaching the surface. This mechanism was first proposed by Kutateladze [20]. Weissman and Ileslamlou [21] proposed that CHF occurs when the volume fraction of vapor in the bubbly layer exceeds a certain critical value. Celata [10] used the Weissman model in order to correlate his own data and found that it needs some improvements.

(b) Liquid film vaporization.

Vapor bubbles grow and connect near the surface to form a vapor blanket and CHF occurs as a result of vaporizing the thin liquid film attached to the wall. This mechanism was proposed by

Lee and Mudawar [26] who tested their model for ΔT_{sub} below 59°C. A similar model was proposed by Katto [22], who tested his model against data with ΔT_{sub} below 117°C.

(c) Overheating at nucleation sites.

At very high heat fluxes, nucleation sites which become locally dry heat up so much during the bubble growth phase that they cannot be rewetted properly after bubble departure.

(d) Temperature of Homogeneous (Spontaneous) Nucleation (THN) limit.

Suppression of nucleate boiling on the coolant wall surface allows very high wall temperatures and CHF based on homogeneous (spontaneous) nucleation. This mechanism was suggested earlier by the present authors [8]. When the wall temperature reaches THN, nucleation occurs spontaneously in the liquid layer near the heated wall. That may lead to the CHF occurrence because under THN conditions the heated wall is covered by a vapor film.

Because of the high potential for suppression of nucleate boiling at high velocity and high subcooling , the first two mechanisms (a) and (b) are not expected to occur in the conditions of interest, namely at high velocity and high subcooling. However, the Katto model for mechanism (b) was found adequate for the conditions reviewed by Celata et al. [23]. Mechanism (a) can happen only at moderate heat fluxes and low subcooling. This mechanism is the dominant one for the familiar saturated pool boiling condition. Whether this occurs in highly subcooled boiling is uncertain as are some details of this mechanism.

Flow instability or flow excursion may induce CHF especially for a system consisting of parallel channels. However this is not a separate CHF mechanism because the physics of the CHF phenomena do not change under these conditions. CHF by one of the above mentioned mechanisms occurs under flow instability conditions as a direct result of flow reduction.

In high heat flux devices thermal wall inertia may play an important role under transient conditions. However, if CHF results are obtained as local heat fluxes under steady state conditions there is no effect due to the thermal wall inertia and CHF results are applicable to tubes or channels with different wall thickness under steady state conditions.

II. EXPERIMENTAL APPARATUS AND COMPUTATIONAL MODELING

II. A. Experimental Apparatus

Experiments under representative non-uniform channel heating conditions have been performed by Hechanova et. al. [11]. Hechanova extracted CHF data from these experiments. Subsequently some of these experiments were analyzed by the present authors for heat transfer data over the entire boiling region to obtain nucleate boiling, CHF and post CHF data.

A copper test section (see Figure 1) was heated on one side by passing an electrical current through a tungsten film (about 0.25 mm thick) which was plasma sprayed over an alumina coating (about 0.1 mm thick) which had itself been sprayed on the copper. The alumina coating electrically insulated the copper test block (19x19x130 mm) from the tungsten. The unheated sides of the test section were insulated. The high velocity coolant flow through a 9.5 mm diameter channel in the center of the copper block was established by a 16-stage centrifugal pump. A stainless ball valve upstream and a needle valve downstream were used to adjust the coolant pressure and velocity.

The incident heat flux (defined in the present study as the power input to the tungsten per unit area facing the copper) is simply determined using the following expression:

$$q_{in} = I \, U \, / \, A_h \tag{8}$$

The hydraulic variables such as coolant pressure, inlet and outlet temperatures, coolant flow rate were measured. A computerized data acquisition system was set up and was capable of reading and storing thermocouple voltages (K-type thermocouples), the flowmeter signal and the electrical power. Five thermocouples were placed at a non-coated side of the test section such that three thermocouples measured axial variations of temperature close to the heater and two

thermocouples measured the temperature at other positions on the wall midsection, as shown in Figure 1.

The experimental data were logged using a data acquisition scanner which eventually creates text files of the data for the thermocouples, flow meter, resistor (heater and shunt) and voltages measurements. The operator controlled the power supply, pump speed, the shunt resistor voltage, and the pressure of the coolant.

The following step-by-step procedure was performed by the operators. It typically took just 10 to 20 minutes to perform and resulted in a steady flow established with known pressure, velocity and inlet bulk coolant temperature. The current to the test section was stepped up slowly by small increments of about 100 A. At a given power level (i.e. after each 100 A current increment), the test section heating was allowed to stabilize (which took on the order of ten to twenty seconds). At this time, the power supply current, shunt resistor voltage, and the power supply voltage were logged. Measurements were taken until component failure due to CHF occurrence (usually accompanied by flashing and/or arcing on the test section heater). The resulting data were: manual readings of power supply voltage, power supply current, shunt resistance voltage, flowmeter readings at the beginning and at the end of test run, and a computer file containing the heater, shunt resistor and five thermocouple voltage measurements versus time.

The total length of the coolant flow path was long (about three meters), the test section was located near the middle of that length. Due to the high subcooling, most of the vapor was condensed shortly after the exit from the heated part of the path. There were no parallel channels and thus no possibility of density wave instability. The test section contribution to the total pressure drop was negligible which eliminated the possibility of a static (Ledinegg) type of instability. That was confirmed by coolant flow rate measurements during experiments, where no variations of mass flux were observed.

The experimental facility was operated within the test parameters given in Table 1.

Table 1. Test parameter range of present study

Parameter Variable	Range	Units
Pressure	1.79 - 3.01	MPa
Inlet temperature	19 - 23	°C
Velocity	3 - 20	m/s
Channel diameter	9.5	mm
Heated length	78	mm

The uncertainty in measurement of the incident heat flux is estimated at 5%. The uncertainty in measurement of the block surface temperature is less than 3°C. The heat transfer coefficients and the coolant side heat fluxes were obtained using these measurements at steady state stages of the power ascension using a special inverse heat conduction modeling technique. This technique is discussed in the next section.

II. B. Computational Modeling

Heat transfer phenomena and representative quantities, such as the heat transfer coefficients, applicable to the coolant side of the test section cannot be calculated directly from the measurements described above. However, the measured heat deposition and outer wall temperature profiles can be used to determine the channel wall heat transfer coefficients by solving the heat conduction problem. Heat conduction in the copper block was analyzed to convert the experimental power input and outer wall temperature measurements to coolant channel wall heat flux distributions and to determine the values of the heat transfer coefficients. The heat conduction axially and azimuthally was determined in a two step one-dimensional analysis in each direction.

In the first step a one dimensional axial heat conduction problem is solved taking into consideration the fact that the copper block is heated along 78 mm in the midsection, with approximately 26 mm long unheated sections on each end of the copper block. This allowed us to estimate the axial peak to average heat flux ratio. The heat transfer from the copper block to the

surroundings was assumed negligible since natural convection to air from the copper surfaces, and conduction to the stainless steel tube fittings provide negligible heat transfer paths given the high conductivity of the copper and the highly effective cooling in the channel. Since the temperature rise in the coolant was at 2 to10 K, and the coolant was 130 to 200 K subcooled, the midplane section is the plane of maximum heat flux. That is why the surface temperatures were measured at the middle and not at the exit of the heated section.

In the second step, the azimuthal peak to average heat flux ratio was estimated considering a one dimensional heat conduction solution with four zones of uniform heat transfer coefficients. This allowed the determination of the azimuthal heat flux peaking factor. The highest heat flux occurs in the zone nearest the heater, and the peaking factor in single phase flow was typically about 1.8 to 2.2. The analysis shows that only the section nearest the heater had channel wall temperatures that exceeded the saturation temperature, given the subcooling of the coolant. Hence, it was assumed that only that section could undergo boiling. With nucleate boiling, the peaking factor may increase since boiling would enhance the overall heat transfer in that zone. Even when film boiling occurred in that section, the typical film thickness is tens of microns and the peaking factor may remain around 1.5.

A single value of the heat transfer coefficient from the wall to the coolant was initially calculated using Equation (1) and that value was then changed until the experimental thermocouple readings of wall temperatures at the midsection position (thermocouples # 1 and 2; see Figure 2) were matched by the calculations. Then for this condition the value of the peaking factor: $pf = q_w/q_{in}$ was calculated (q_{in} = heat deposition per unit area at the copper-alumina interface and q_w = heat flux at the coolant-wall interface closest to the alumina (W/m^2)). The test section was divided into three zones (see Figure 2), with zone #1 being the zone at the heated side of the block and zone #3 being the opposite side.

For zone#1, the channel wall heat flux (q_w) was calculated as:

$$q_w = q_{in}\, pf \qquad\qquad (9)$$

It was assumed that the values of the heat transfer coefficients for zones #2,3 are equal to each other ($h_2 = h_3$). Calculations showed that no boiling occurs in zones #2,3 since T_w remained below T_s. For low values of the incident heat flux and for $T_w < T_s$ for zone #1, the heat transfer coefficient for this zone (h_1) was assumed equal to the values for zones #2, 3, or in other words $h_1 = h_2 = h_3$. For these conditions ($T_w < T_s$ for all zones) the heat conduction equation was solved and the values of the heat transfer coefficient was obtained with which the block surface temperature and the reading of thermocouple #2 matched. An assumption was made that when $T_w > T_s$ for zone #1 (nucleate boiling in zone #1) h_2 and h_3 remain at the same values as they had for $T_w < T_s$ for the same coolant velocity. For this condition (nucleate boiling in zone #1) the heat conduction equation was solved and the value of h_1 (nucleate boiling heat transfer coefficient) was obtained for which the calculated value of the block surface temperatures at the position of thermocouples #1 and 2 were matched. Thus the values of heat transfer coefficients for both single-phase region and nucleate boiling region for the midsection location were obtained. The midsection here has a special significance since it is the plane where there is the maximum channel wall heat flux in comparison with other parts of the test section (due to heat conduction within the copper block).

The analysis method created was validated against HEATING7.2 [12] (3D, finite difference) computer code, as well as against theoretical calculations of simple problems. By comparison to three-dimensional heat conduction HEATING7.2 [12] calculations, it was found that the uncertainty in the calculated values of heat transfer coefficients for a single-phase region is 17% and for nucleate boiling region is 21%. A comparison between the results of the model used in this study and the HEATING7.2 results is presented in Figure 3. It can be seen that good agreement exists between the two analyses at the hottest part of the wall, while only a fair agreement exists in the cold region of the wall.

In order to evaluate how possible errors in thermocouple readings influence the values of heat transfer coefficients obtained from calculations, a sensitivity analysis was performed. It was found that a 1% error in thermocouple reading of block surface temperature (maximum possible

error) produces about the same error in the value of heat transfer coefficient for a single-phase condition and about 1.5% error for a two-phase condition.

The midsection wall temperature and coolant bulk temperature are used to obtain the local heat flux. No account is taken of developing velocity and coolant temperature distributions. This is done in order to simplify the problem (it should be an acceptable approximation with the present geometry). Because only high water velocities are considered in this study, the flow is highly turbulent. The thermal entrance effects for cold water (20°C) entering the test section would be minimal because water at this temperature has a relatively high Prandtl number (about 7). Data presented in [17] show that for Re = 100,000 the heat transfer coefficient for a single-phase region is expected to be less than 10% higher than for a fully developed flow, well within the ±17% uncertainty of the experimental technique. Hence, the thermal entrance effects can be neglected. There should be no thermal entrance effects for the nucleate boiling region.

III. RESULTS

III. A. Single-phase region

For the single-phase convection region (no boiling occurred within the entire perimeter of the test section) it was found that the Petukhov correlation (Equation (1)) with a viscosity correction multiplier provides excellent agreement with experimental results. Experimental and theoretical results are shown in Figure 4. It is possible to obtain high local heat fluxes (up to 35 MW/m^2 for flow velocity of 20 m/s) at high subcooling without getting into nucleate boiling. A comparison of experimental values of heat transfer coefficients for the single-phase region with the values obtained form the Petukhov correlation are in agreement within ± 15%. Because of the good agreement of the experimental data in the single-phase region with the Petukhov correlation, it was concluded that the present study computational modeling and data reduction method are reliable.

III. B.   Nucleate boiling region

It was found that none of the correlations described above (Equations (2)-(7)) adequately describe the experimental results for nucleate boiling conditions at high heat and mass fluxes (see Figures 5 and 6). The Jens-Lottes correlation (Equation (2)) over-predicts the values of heat transfer coefficients for the present flow conditions. This is not surprising because it was derived for moderate flow velocity where there is no suppression of nucleate boiling. Yin's correlation (Equation (3)) under- predicts the present experimental results because it was derived for a smaller tube diameter (3.5 mm) where the degree of nucleate boiling suppression is higher according to [9]. Experimental results of the present study show that Shah's and Chen's correlations are quite correct for low velocities (V<5 m/s) but over-predict the heat transfer coefficients for higher velocities. The Shah correlation does not take into consideration nucleate boiling suppression, exhibited in some of the experiments. While the Chen correlation predicts nucleate boiling suppression, it does not predict the right slope of the wall heat flux versus wall superheat.

A new nucleate boiling correlation applicable to such conditions is needed. Experimental results showed that the Chen correlation (Equations (4)-(6)) is one of the better choices when compared with other correlations for subcooled nucleate boiling. However, because it was originally derived for saturated flow boiling, alternative corrections are needed for the suppression factor (S) and for the correction multiplier (F) in the forced convection term, which allows for the enhancement of heat transfer mechanisms arising from the generation of vapor in the boundary layer next to the wall. Thus the F factor should be a function of the S factor and wall temperature.

An assumption can be made that there are two mechanisms for nucleate boiling suppression. The first mechanism is due to the turbulence influence on steam bubble growth [8, 9, 13] for high velocity flows. For this case turbulent velocity oscillations can be very high [9] and the probability of turbulent vortices destroying vapor bubbles on the wall gets larger as the flow velocity increases. The second mechanism is due to the high heat flux. Although the total

population of nucleation sites increases with increasing wall heat flux, the startup of new sites deactivates many of the sites active at lower wall heat flux (lower superheat). So the total suppression factor in the nucleate boiling term is a function of both Reynolds number and heat flux, thus:

$$S = S_v \ S_q \tag{10}$$

where S_v is a decreasing function of the Reynolds number and S_q is a function of the heat flux ratio to CHF (see Equation (23)). Given all of these factors the following form of the correlation is proposed:

$$q_w = F \ h_{sp} \ (T_w - T_b) + S \ h_{nb} \ (T_w - T_s) \tag{11}$$

where h_{sp} is to be calculated using Equation (1) with a viscosity correction multiplier and h_{nb} is to be calculated using Equation(6). Correlations for the F and S coefficients were found using experimental results. F takes the form:

$$F = (36.7S_v^{1.06} - 37.2S_v^{0.5} - 14.5\exp(S_v) + 37S_v^{0.16})\left(\frac{T_w}{T_s}\right)^2 \tag{12}$$

Equation (12) can be applied for a velocity range $V = 4.4$ to 15 m/s ($Re = 4.2 \cdot 10^4$ to $1.4 \cdot 10^5$). For $V < 4.4$ m/s ($Re < 4.2 \cdot 10^4$), $F = 0$. Therefore, for low velocities there is no nucleate boiling suppression and many vapor bubbles are generated on the heated wall. They destroy the boundary layer and prevent heat transfer via convection. S takes the form:

$$S = S_v \ S_q = \frac{1}{1 + 1.52 * 10^{-16}(Re)^{3.37}} * \frac{1}{1 + 1.41\left(\dfrac{q_w}{CHF}\right)^{29}} \tag{13}$$

For the value of CHF in Equation (13) results presented in the next section of this paper (Equation (23)) are used. The ratio of $\dfrac{q_w}{CHF}$ has to be always less than one. For $\dfrac{q_w}{CHF} < 0.85$, S_q can be assumed to be equal to one and, thus, CHF value is not needed in order to compute the value of heat transfer coefficient for nucleate boiling region.

Comparisons between the proposed correlation and experimental results for velocities V = 4.34 and 10.2 m/s, P = 3 MPa, T_b = 293 K are shown in Figures 5 and 6.

The agreement between the calculated and experimental results was found to be in the range of ± 20% for P = 3 MPa, T_b = 290 to 295 K and V = 3-15 m/s (Figure 7). The proposed correlation can be applied only if it predicts a wall heat flux higher than possible by single phase convection: $q_w > h_{sp}$ (T_w - T_b); otherwise Equation (1) should be applied.

III. C. Critical Heat Flux Region

In order to verify the second possible mechanism (see (b) in Introduction) the CHF data points are plotted in Figure 8 as Stanton number versus Peclet number. These coordinates also display the Saha and Zuber bubble departure criterion [14] that distinguishes between the hydrodynamically-controlled and thermally-controlled bubble departure regions. These regions are distinguished using the Peclet number. The Onset of Significant Voids (OSV) or bubble departure is determined using the Nusselt or Stanton numbers as follows:

$$Pe = \frac{GDc_{pf}}{k_f} \tag{14}$$

$$Nu = \frac{q_w D}{k_f (T_s - T_b)} \tag{15}$$

$$St = \frac{q_w}{Gc_{pf}(T_s - T_b)} \tag{16}$$

For Pe < 70,000, bubble departure is thermally-controlled and occurs when Nu > 455.

For Pe > 70,000, bubble departure is hydrodynamically-controlled and occurs when St > 0.0065.

It is clear from Figure 8 that all data points except those for very low velocity (V < 0.6 m/s) fall below the line St = 0.0065. Hence, according to the Saha-Zuber criterion, vapor bubbles are not expected to leave the surface. Furthermore, in such a highly subcooled coolant with a thin thermal boundary layer, the ability of a bubble layer to exist away from the wall is doubtful since any vapor that forms should condense very close to the wall. The bubble departure criterion is

surpassed only for low velocity flow data (V < 0.6 m/s). For these cases the thermal boundary layer has a much better opportunity to develop and behave as suggested by Celata [10]. CHF predictions for these low velocity cases found by Hechanova [11] suggest that this mechanism (b) for CHF is plausible in that region.

It seems possible that mechanism (c) for CHF can occur when nucleate boiling is suppressed and wall temperatures are high, but below THN. For this case bubbles stay on the heated wall, but their total number is small because of nucleate boiling suppression. Thus, they cannot form a bubble layer near the wall and they also cannot prevent subcooled liquid movement toward the heated surface. Thus, if the wall temperature is below THN, the only possible mechanism is overheating at nucleation sites, i.e. mechanism (c).

Figure 9 shows the maximum inner wall temperature as a function of flow velocity. The figure also shows the spontaneous nucleation temperature ranges (J is spontaneous nucleation rate per unit volume). From this figure it is clear that for velocities less than 10 m/s the inner wall temperature is high but below THN. Hence, the only possible mechanism for this case is overheating at a nucleation site. However, for velocities greater than 10 m/s, the inner wall temperature exceeds THN. Thus, for these cases CHF is likely to be due to the THN limit, i.e. mechanism (d) (see Introduction). When the wall temperature reaches THN, nucleation occurs spontaneously in the liquid even with a complete absence of nucleation sites on the heated wall.

Using Equations (11) to (13), CHF due to THN can be determined as follows:

$$CHF_{THN} = F\ h_{sp}(THN - T_b) + 0.41S_v h_{nb}(THN - T_s) \qquad (17)$$

Predicted CHF values due to THN and the CHF data points are plotted in Figure 10. Two methods of analysis have been used to obtain local critical heat flux values from the recorded data. Seven data points in the present study (present study CHF data points) are deduced from the measurements using computational modeling described above. These seven CHF data points deduced from the measurements using another type of modeling (HEATING7 code with the Petukhov correlation for single-phase flow and the Shah correlation for nucleate boiling region) are also shown in Figure 10 (Hechanova [11] data used in this study). The two analysis methods

give somewhat different results as can be seen in Figure 10. It is felt that the methods of the present paper are better than those used by Hechanova [11] because of the advantages of the present paper methodology already discussed in the Computational Modeling section. Other Hechanova CHF data points for which present computational modeling have not been used are also shown in Figure 10 (Hechanova [11] data not used in this study).

It is clear from this figure that CHF predictions of Equation (17) are reasonable. Data extrapolations from the Canadian look-up table [16] cannot be used for this range of velocities. The CHF mechanism here is different from that for the range of velocities in the data of the look-up table. It is obvious from this figure that the Canadian look-up table [16] can be used for CHF predictions for velocities below 5 m/s, and Equation (17) can be used in the range of velocities greater than 11 m/s. The question remains: "What correlation should be applied in the intermediate range of velocities?" The answer to this question will be developed next.

Let us assume that the local wall heat flux is greater than CHF. In other words, let us consider the post-CHF region in which high velocity, low temperature liquid is present in the center of the channel, and the wall is covered by a thin film of vapor. For this case the local wall heat flux can be represented in the form of a sum:

$$q_w = q_g + q_l \tag{18}$$

where at the liquid-vapor interface: q_g is heat flux due that causes evaporation; q_l is heat flux that enters the liquid by convective heat transfer, and heat transfer by radiation is neglected.

For the general case, the heat flux into the subcooled liquid (q_l) can be determined as:

$$q_l = h_c(T_s - T_b) \tag{19}$$

where h_c is an appropriate heat transfer coefficient. That coefficient is likely to be enhanced above those obtained from typical correlations for turbulent flows. The vapor-liquid interface is expected to be irregular from waves and from the agitation produced when evaporation occurs.

There seems to be no defensible way of estimating the enhancement. A possible approach would be to use a type of Reynolds analogy if appropriate measurements of pressure drop were available. Since it seems that no such measurements exist, we have chosen to use known pressure

drop enhancement observed in a different physical situation (subcooled flows in the presence of nucleate boiling on the heated channel walls). An expression to represent such pressure drop enhancement is recommended for use in Russian codes [17] and has the following form:

$$\frac{\Delta P_{nb}}{\Delta P_{sp}} = 1 + 5.38 \left(\frac{q_w}{H_{fg} \rho_g V} \right)^{0.7} \qquad (20)$$

Now we shall assume that the vapor-liquid interface in film boiling plays the role of the heated wall in nucleate boiling. Because the interface is rough, bubbles can leave this film in the transverse direction. Hence, we apply Equation (20), assuming that ΔP_{sp} is the value of pressure drop in the case where there is no vapor flow from the liquid-vapor interface inside the bulk liquid and ΔP_{nb} is the value of pressure drop when there is transverse vapor flow inside the subcooled liquid. With the assumption that the Reynolds analogy is valid for our case, the pressure drop ratio in Equation (20) is the same as the heat transfer enhancement factor. Thus the heat transfer coefficient in Equation (19) can be determined as:

$$h_c = \left(1 + 5.38 \left(\frac{q_l}{H_{fg} \rho_g V} \right)^{0.7} \right) h_{sp} \qquad (21)$$

where: h_{sp} = single-phase heat transfer coefficient, evaluated using Equation (1).

With the use of Equations (19) and (21), the heat flux removed by subcooled liquid from a vapor film can be calculated as follows:

$$q_l = h_{sp} \left(1 + 5.38 \left(\frac{q_l}{H_{fg} \rho_g V} \right)^{0.7} \right) (T_s - T_b) \qquad (22)$$

Equation (22) has been used to obtain values of heat flux transferred to the subcooled liquid. Those values are identified as the heat flux limit for subcooled liquid and are presented in Figure 10. It is interesting that for low velocities ($V < 4$ m/s) this heat flux is lower than calculated from the Canadian look-up table [16] for CHF, but for high velocities this heat flux is higher than CHF. Thus, if $q_l > q_w$ > CHF, then a non-steady state condition will exist on a heated wall. Because the wall heat flux exceeds CHF, we have film boiling. But, vapor penetration into the

subcooled liquid increases heat transfer and the heat flux removed from vapor becomes greater than the wall heat flux. Hence, the vapor in the film will condense. When there is no vapor film, there is no heat transfer enhancement, and a wall heat flux greater than CHF occurs with film boiling again. So, the only possibility to get stable film boiling on a heated wall is to exceed the value of subcooled liquid heat flux (Equation (22)). Hence, another limit exists, designated the heat flux limit for subcooled liquid. Only when the wall heat flux is greater than this limit can we have stable film boiling on a heated wall.

Two regions of film boiling can exist in some cases for high velocities and high subcooling. In the first region (region AB in Figure 11) an unsteady state film boiling exists. In this region, as was stated before, we have subcooled liquid vaporization and vapor film condensation. This region can exist only when $q_l > q > CHF$.

But when $q > CHF > q_l$, a stable film boiling can exist on a heated wall (region BC in Figure 11). In comparison with the previous region, there is no steam condensation in this region. Thus we should expect some reduction in the heat transfer coefficient which may cause overheating of a tube. If $q_l < CHF$ we should have only this film boiling region (classical film boiling). These regions are shown in Figure 11.

Figure 10 also shows the CHF data. Now it becomes clear why the Canadian look-up table [16] does not give correct CHF values. The CHF data points may represent post-CHF data points. Since the vapor film is stable only when the Heat Flux Limit for Subcooled Liquid is reached, it is difficult to determine CHF from thermocouples readings and we have an apparent CHF disappearance. In other words there is no sharp reduction in the heat transfer coefficient because of the transition from nucleate to film boiling. By CHF occurrence we mean the transition from single-phase convection plus nucleate boiling to film boiling.

The question remains: "Why are data points for high velocities ($V > 11$ m/s) below the Heat Flux Limit for Subcooled Liquid? " A possible explanation is that Equation (22) is derived on the assumption that the Reynolds analogy is valid. Also it is based on Equation (20) which was not

derived for extremely high velocities. Equation (22) is recommended only for water pressure greater than 1 MPa.

The maximum heat flux for nucleate boiling is proportional to $E_{nb} h_{sp} (T_w - T_b)$, where E_{nb} is the enhancement ratio for nucleate boiling region ($E_{nb} = h_{nb}/h_{sp}$). If we compare the last expression with Equation (22) it is clear that, in order to have $q_l > CHF$, the enhancement factor for film boiling (E_{fb}) must be greater than the enhancement factor for nucleate boiling region (E_{nb}). For low velocities there is no nucleate boiling suppression, and a large nucleation rate causes a very high E_{nb}. For high velocities there is nucleate boiling suppression. At extremely high heat flux a vapor film on the heated wall begins to play the role of a vapor source. In other words the heat transfer rate of film boiling is enhanced and at high heat fluxes and velocities it is enhanced to values greater than nucleate boiling before CHF occurrence.

IV. DEVELOPMENT OF CHF CORRELATIONS

The preceding subsections indicate that different mechanisms may control the CHF occurrence at different flow velocities. The following procedure is recommended to assess heat flux limits. First, the likely CHF mechanism should be determined. This can be done with the help of the Canadian look-up table [16] and Equation (17) for the THN type of CHF. The Canadian look-up table provides CHF values caused by overheating at a nucleation site - CHF_{OV}. Equation (17) provides CHF due to the THN limit. Comparison of these two heat fluxes (CHF_{OV} and CHF_{THN}) should be made over the whole flow velocity range. The critical heat flux equals the minimum of these two heat fluxes:

$$CHF = Minimum \{ CHF_{OV}, CHF_{THN} \} \qquad (23)$$

Note that the Canadian look-up table [16] covers all possible values of subcooling, but flow velocities only up to 7.5 m/s. It is assumed here that extrapolations may be done for velocities greater than 7.5 m/s.

A local heat flux limit (q_{limit}) for the wall is obtained by assuming that the larger of the two physical heat transfer mechanisms can sustain reasonable temperatures even if the other mechanism is no longer effective. T2

That is,

$$q_{limit} = \text{Maximum} \{ CHF, q_l \} \tag{24}$$

The results of this procedure are shown in Figure 12 for $P = 3$ MPa. Note that Figure 12 is a modified version of Figure 10. It is clear from Figure 12 that the recommended procedure predicts reasonable results (within $\pm$ 20%) for the heat flux limit. Once this limit is reached a wall temperature excursion to much higher values is expected.

The proposed procedure for heat flux limit evaluation was applied not only to CHF data analyzed in the present study, but also to CHF data presented in [11]. The data show good agreement with the proposed procedure, since the data fall within $\pm$25% of the predicted value, 75% of the data falls within $\pm$20% of the predicted value.

V. CONCLUDING REMARKS

For the single-phase region, the Petukhov correlation (Equation(1)) was found to be applicable. A subcooled boiling correlation for high mass flow rate and high heat flux conditions has been proposed. It is based on the Chen nucleate boiling and convective terms with modified suppression and enhancement factors. The new correlation was found to be more reliable than any of the other correlations tested for nucleate boiling. Since the proposed correlation distinguishes between the nucleate boiling and forced convection effects, it can be used in assessing the suppression of nucleate boiling which exists at high velocities and for prediction of the THN limit at the channel wall.

A new procedure is recommended for evaluating the limiting heat flux in highly subcooled flow. A CHF can occur when the wall temperature reaches the THN limit. This occurs at high velocity flow which suppresses nucleate boiling. Equation (17) is proposed to calculate CHF

due to THN limit. Such CHF can occur without accompanying high wall temperatures. Only after exceeding the Heat Flux Limit for Subcooled Liquid in the post-CHF region are high wall temperatures expected. Equation (22) is recommended in order to evaluate the Heat Flux Limit for Subcooled Liquid in post-CHF region. In some cases this heat flux can be a real limit.

When the inner wall temperatures are below the THN value, CHF occurs due to overheating at a nucleation site. The Canadian look-up table [16] is recommended for this case.

Equations (23) and (24) are proposed in order to evaluate the heat flux limit for high velocity flows. However, continuing validation and improvement of CHF correlations are still necessary. So is the development of new physically based correlations and the collection of new relevant data bases.

REFERENCES

1. Boyd, R. D. and Meng, X., "Local heat transfer for subcooled flow boiling with water." *Fusion Technology,* **22**, 12-15, 1992.

2. Jens, W. H. and Lottes, P. A., "Analysis of heat transfer, burnout, pressure drop and density data for high pressure water." ANL-4627, 1951.

3. Yin, S. T., "Prediction of highly subcooled flow boiling for cooling of high heat-flux components in fusion reactors." *Proceedings of the NURETH-6 Conference,* Grenoble, 17-27, 1993.

4. Chen, J. C., "A correlation for boiling heat transfer to saturated fluids in convective flow." *ASME Paper,* no.63-HT-34, 1963.

5. Butterworth, D., "Unresolved problems in heat exchanger design." *Inst. of Chem. Eng. Symp. Ser.,* **60**, 231-248, 1980.

6. Dittus, F. W. and Boelter, L. M. K., Publ. Eng., University of California, 2:443, Berkeley, 1930.

7. Shah, M. M., "A general correlation for heat transfer during subcooled boiling in pipes and annuli." *ASHRAE Transactions,* Part 1, **83**, 1-8, 1987.

8. Lekakh, B. M., Meyer, J. E. and Kazimi, M. S., "Mechanisms for extreme heat transfer conditions in water-cooling of fusion reactor components." *Fusion Engineering and Design,* **28**, 59-62, 1995.

9. Vasil'ev, A. N. and Kirillov, P. L., "On the possibility of breakup of vapor nuclei by turbulent eddies." *High Temperature,* **13**, 1118-1120, 1975.

10. Celata, G.P., "Rationalization of Existing Mechanistic Models for the Prediction of Water Subcooled Flow Boiling Critical Heat Flux." *Int. J. Heat Mass Transfer,* Suppl.1, **37**, 373-380, 1994.

11. Hechanova, A. E., Kazimi, M. S. and Meyer, J. E., "A framework for critical heat flux prediction in high heat flux components." *Proceedings of the High Heat Flux Thermal Management session of the 1995 International Mechanical Engineering Congress and Exposition,* San Francisco, CA, 12-17, 1995.

12. HEATING Version 7.2b, Heat Conduction Code: 3D Conduction Profile. Computing Application Division, Oak Ridge National Laboratory, 1993.

13. Kudryavtsev, I. S. and Lekakh, B. M., "Nucleate boiling of water in twisted tape swirled flow." *Heat Transfer - Soviet Research,* **22**, 705-712, 1990.

14. Saha, P. and Zuber N., "Point of Net Vapor Operation and Vapor Void Fraction in Subcooled Boiling," *Proceedings 5th International Heat Transfer Conference,* Tokyo, 17-27, 1974.

15. *Thermophysical Properties of Liquids in the Metastable (Superheated) State*, McGraw-Hill, N.Y., 417, 1988.

16. Groeneveld, D.C., "1986 AECL-UO Critical Heat Flux Look up Table." *Heat Transfer Engineering*, **7**, 46-62, 1986.

17. *Codes of Thermohydraulic Calculations for Nuclear Power Plants* (in Russian), St. Petersburg, NPO TsKTI, 1986.

18. Simon-Tov, M., Gambill, W, Nelson W., "Thermal-Hydraulic Correlations for the Advanced Neutron Source Reactor Fuel Element Design and Analysis." 1991 ASME Winter Annual Meeting, Atlanta, 1991.

19. Inasaka, F., Nariai, H., "Critical heat Flux of Subcooled Boiling with Water for High Heat Flux Application." *High Heat Flux Engineering II,* 1989.

20. Kutateladze, S.S., *Izv. Akad. Nauk SSSR Otd. Tekh. Nauk,* (in Russian), **4**, 529-536, 1951.

21. Weissman, J. and Ileslamlou, S., "A Phenomenological Model for Prediction of CHF under Highly Subcooled Conditions." *Fusion Technology,* **13**, 1988.

22. Katto, Y., "Prediction of CHF Subcooled Boiling in Round Tubes." *Int. J. Of Heat & Mass Tran.,.***33**, 9, 1921-1928, 1990.

23. Celata ,G.P., Cumo, M., and Mariani, A., "Assessment of Correlations and Models for the Prediction of CHF in Water Subcooled Flow Boiling." *Int. J. Heat Mass. Transfe*r, **37** (2), 237-255, 1994.

24. Nariai, H., Inasaka, F., Ishikawa, A., and Fujisaki, W., "Critical Heat Flux of Subcooled flow boiling in tube with internal twisted tape under non-uniformed heating conditions." *Proceeding of the 2nd JSME-KSME Thermal Engineering Conference,* **3**, 285-288, 1992.

25. Gaspari, G.P., "Comparison among data of electrically and e-beam heated tube.*" Proc. 3rd Int'l Workshop in High Heat Flux Components Thermal-Hydraulics in Fusion Reactors,* Cadarach, 1993.

26. Lee, C.H., and Mudawar I., "A Mechanistic Critical Heat Flux Model for Subcooled Flow Boiling based on local bulk flow conditions." *Int. J. Multiphase Flow* **14**, 711-728, 1988.

27. Kinoshita, H., et al, "Study on the Mechanism of Critical Heat Flux Enhancement for Subcooled Flow Boiling in a Tube with Internal Twisted Tape under Nonuniform Heating Conditions." *Heat Transfer* - Japanese Research, **25**, 299, 1996.
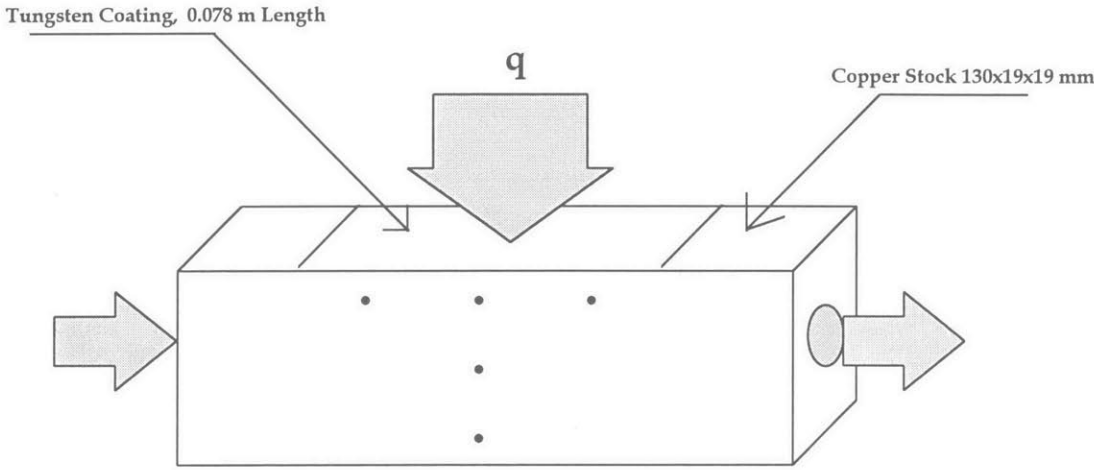
FIGURES

Tungsten Coating, 0.078 m Length

q

Copper Stock 130x19x19 mm

Figure 1: Test section sketch, showing placement of the thermocouples

$(q_o")*pf_x$

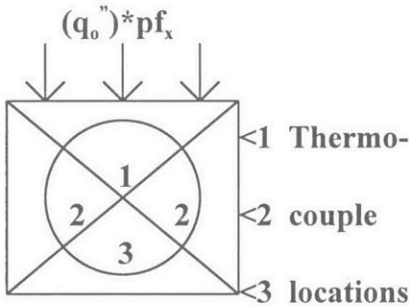<1 Thermo-

1

2   2   <2 couple

3

<3 locations

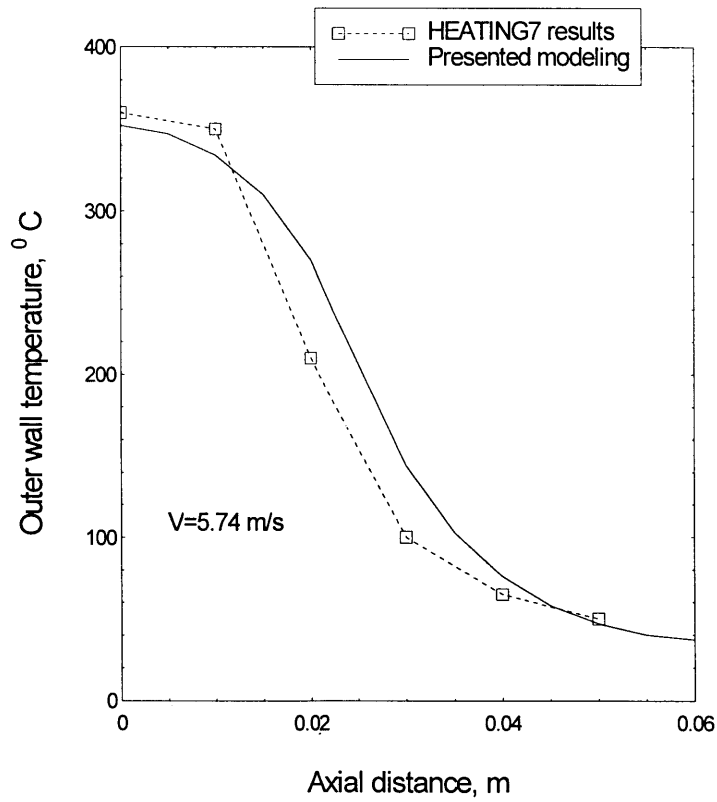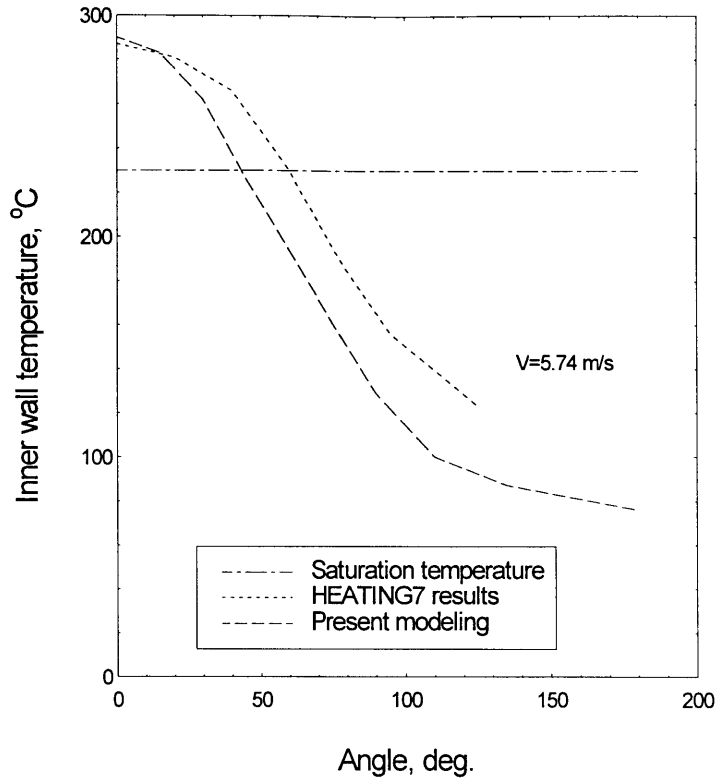**Figure 2: Test section cross section specifications for calculational model.**

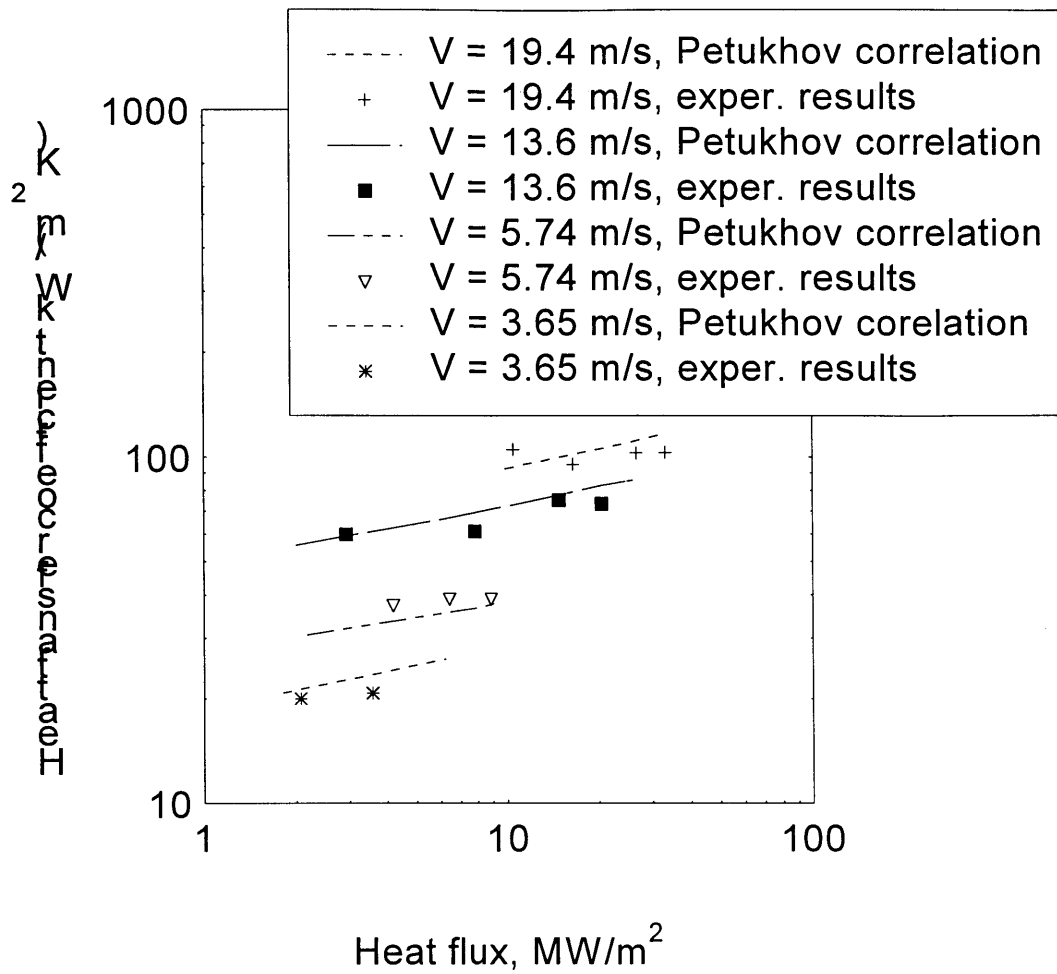**Figure 3: Comparison between HEATING7 and present computer modeling**

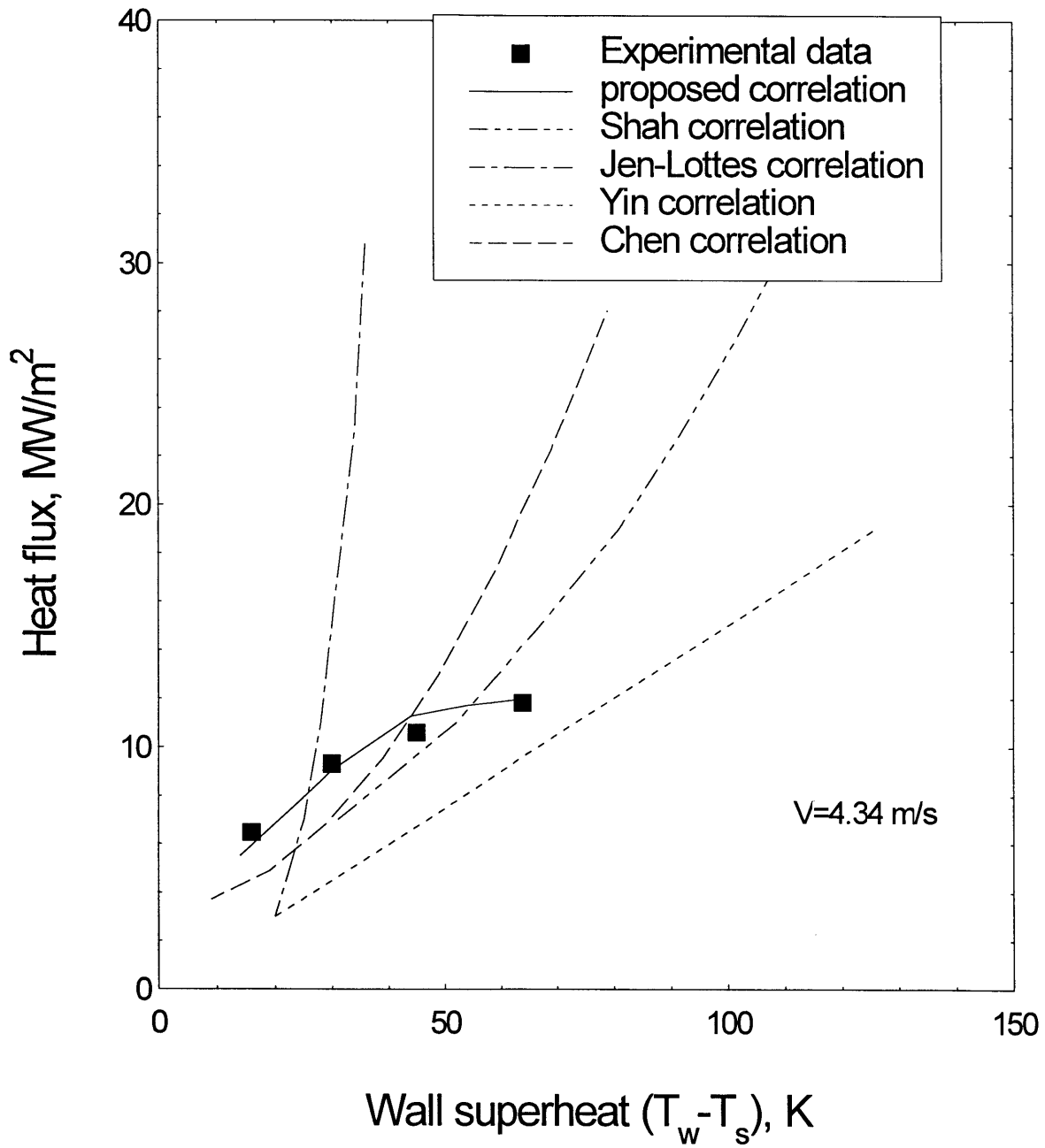**Figure 4: Heat transfer coefficient as a function of local heat flux.**

Figure 5: Local heat flux as a function of wall superheat
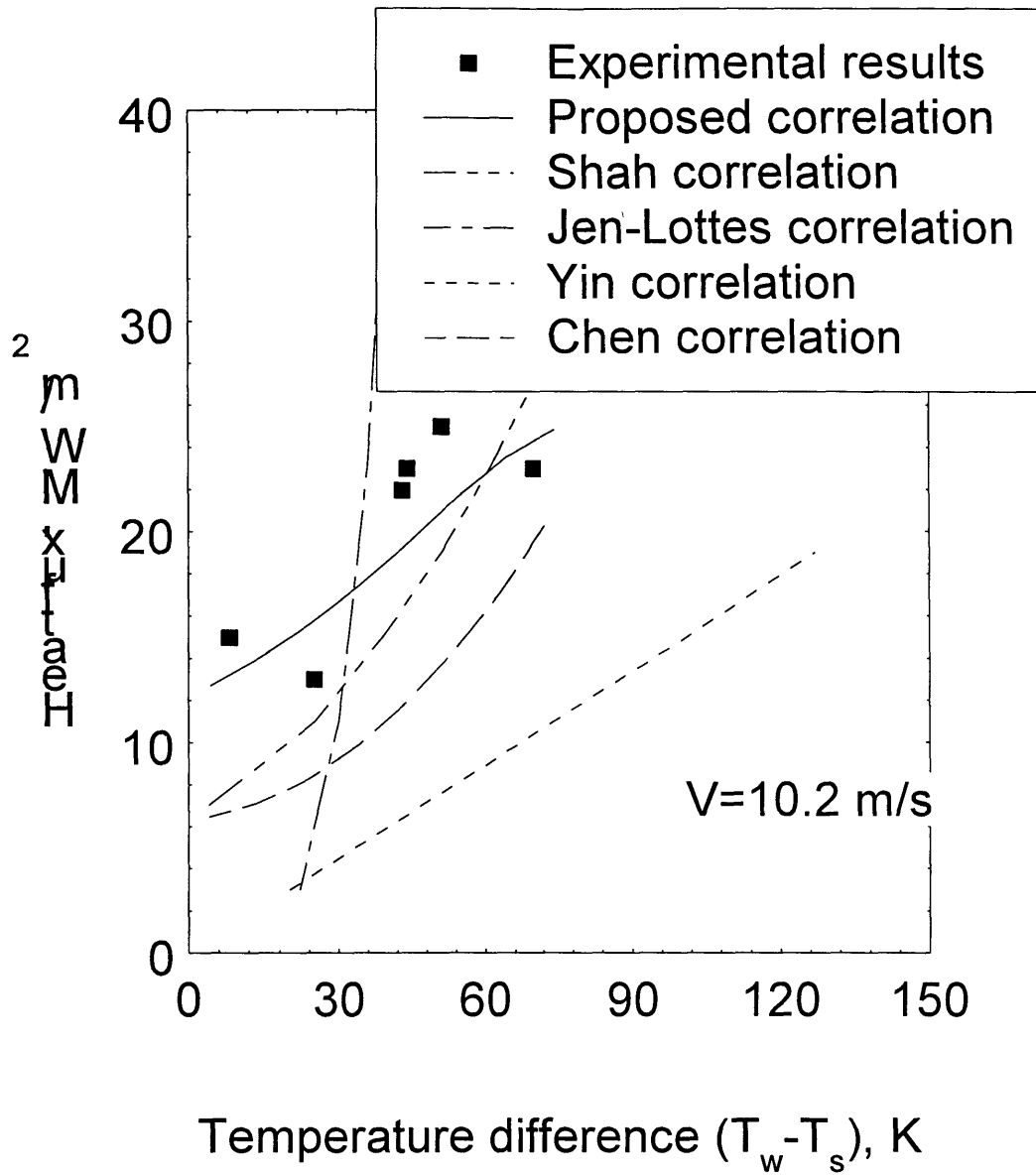
Figure 6: Local heat flux as a function of wall superheat.
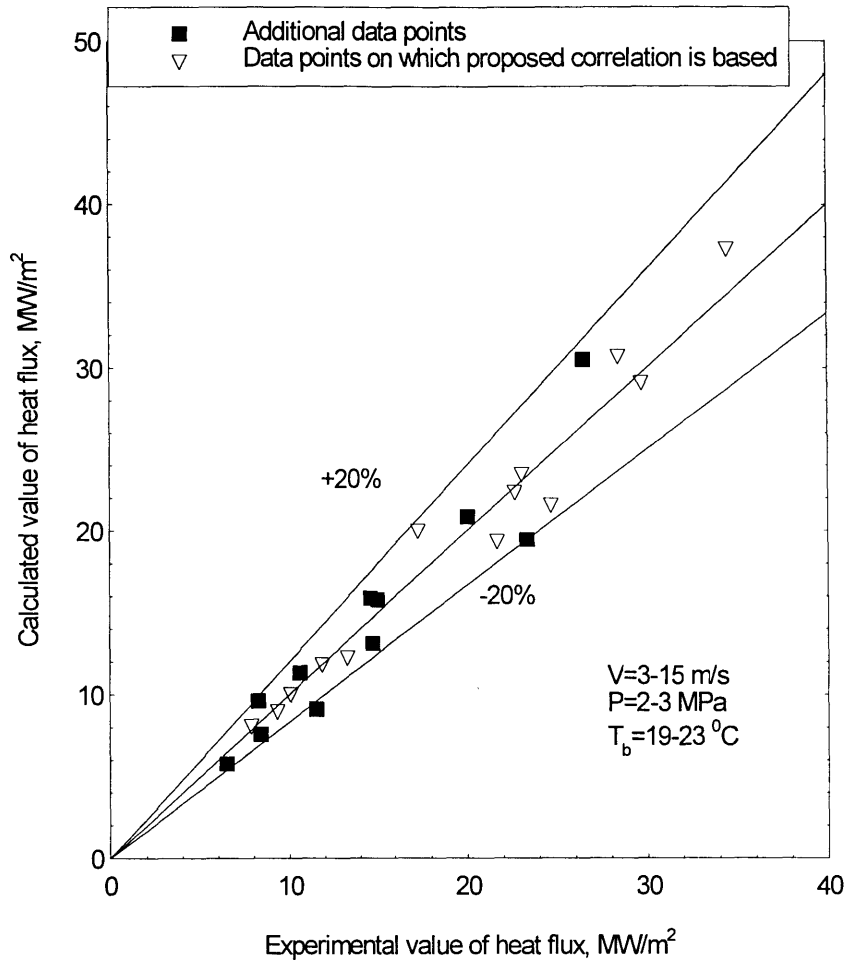
Figure 7: Comparison between experimental and calculated results
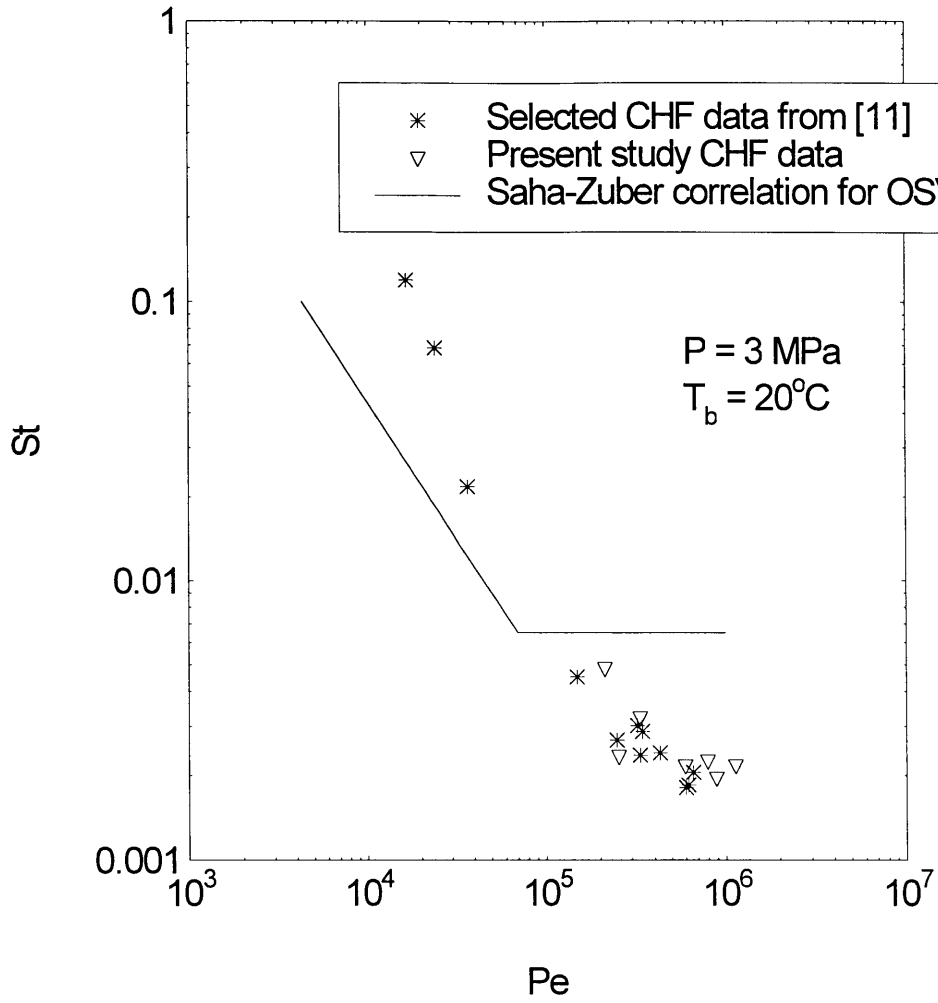
Figure 8: Stanton CHF number as a function of Peclet number
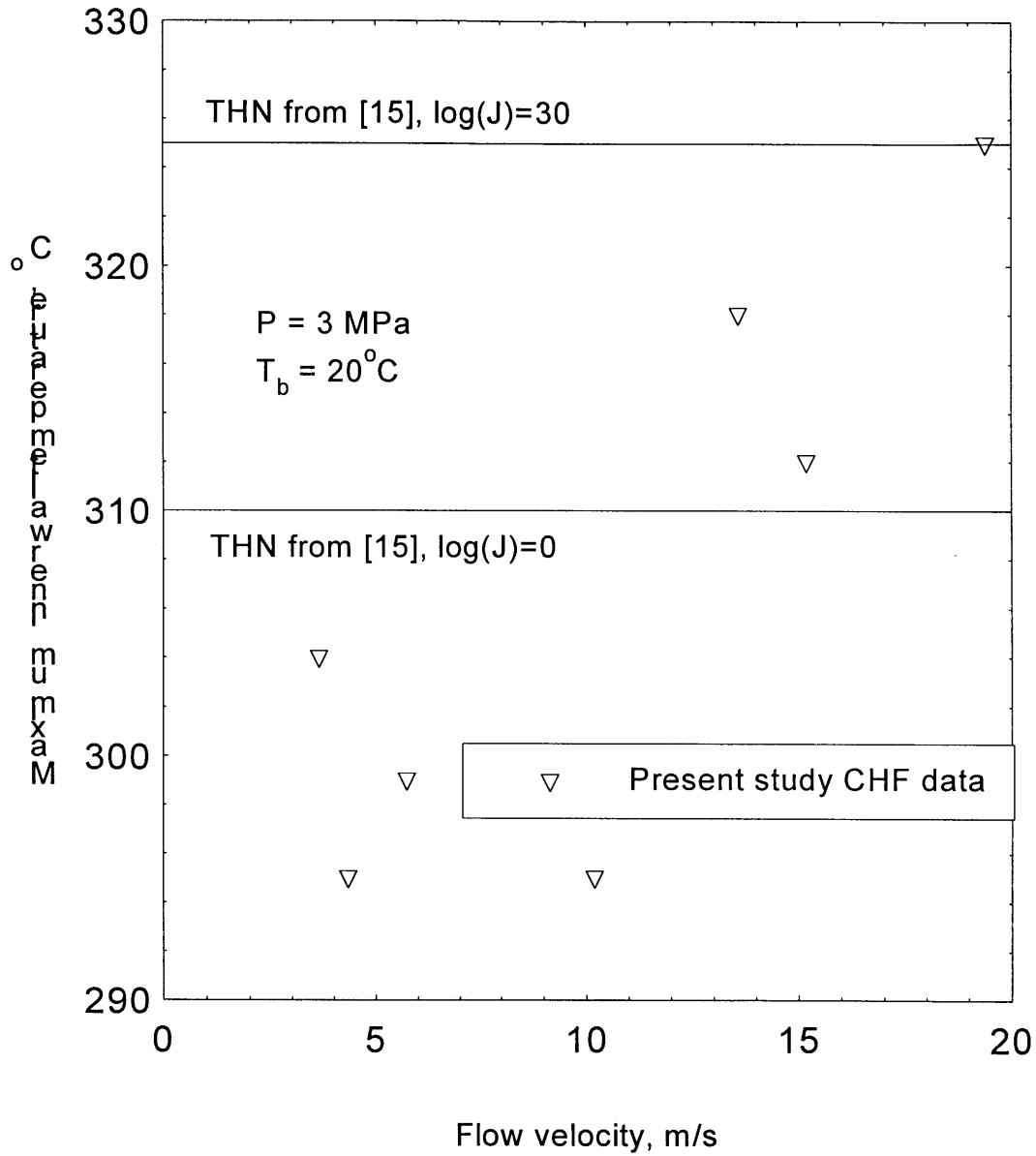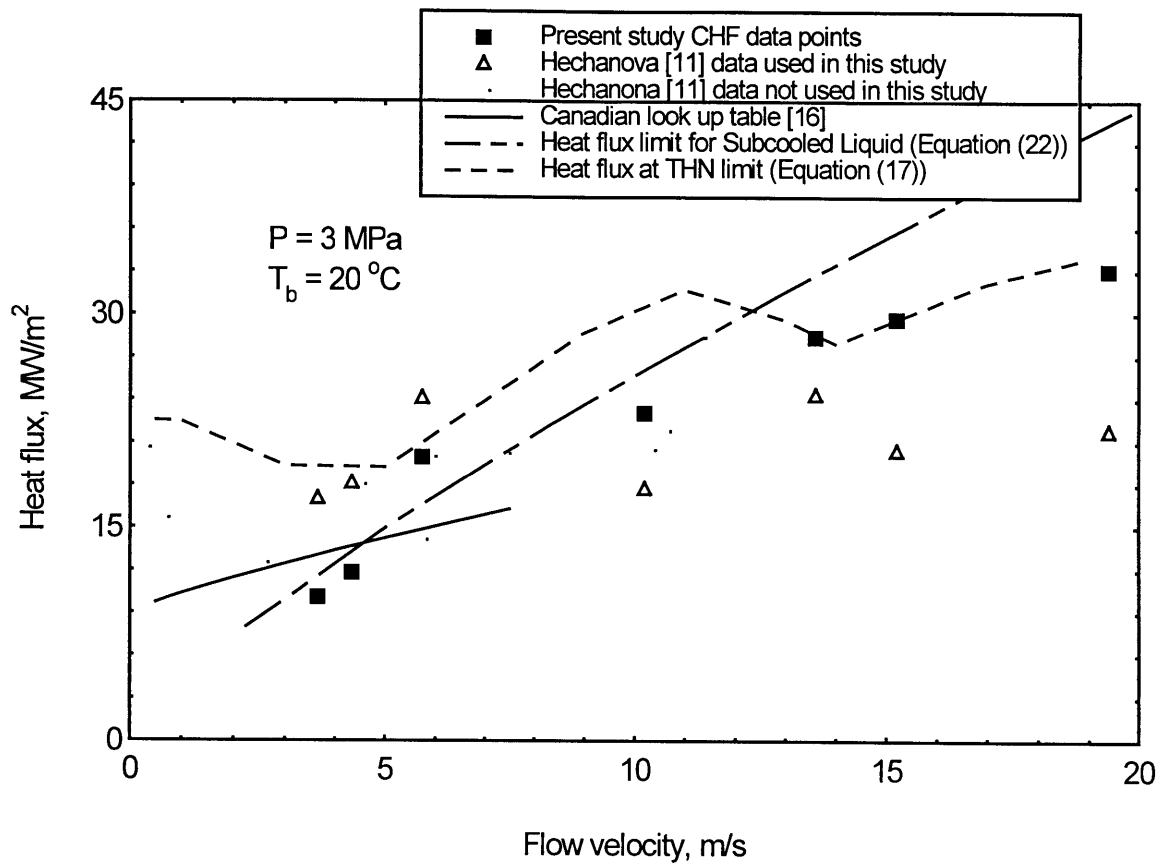
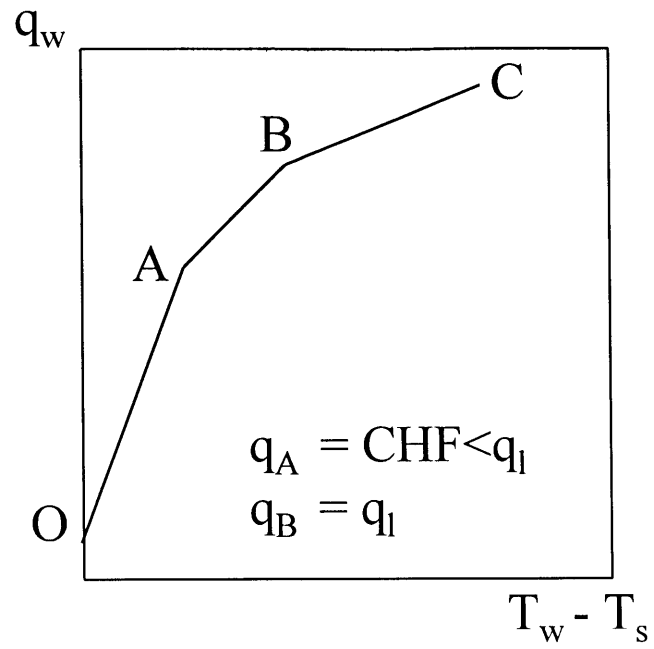**Figure 9: Maximum inner wall temperature as a function of flow velocity**

Figure 10: Local critical heat flux as a function of flow velocity

Figure 11: Film boiling regions
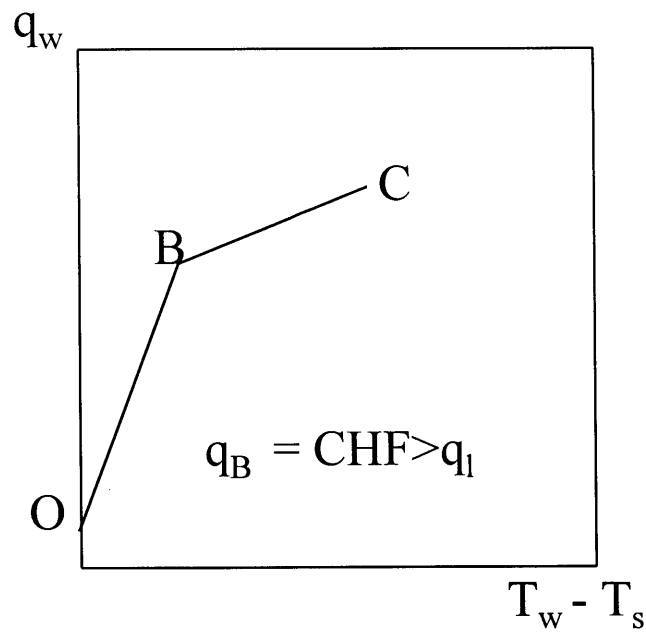
OA(OB) - nucleate boiling region

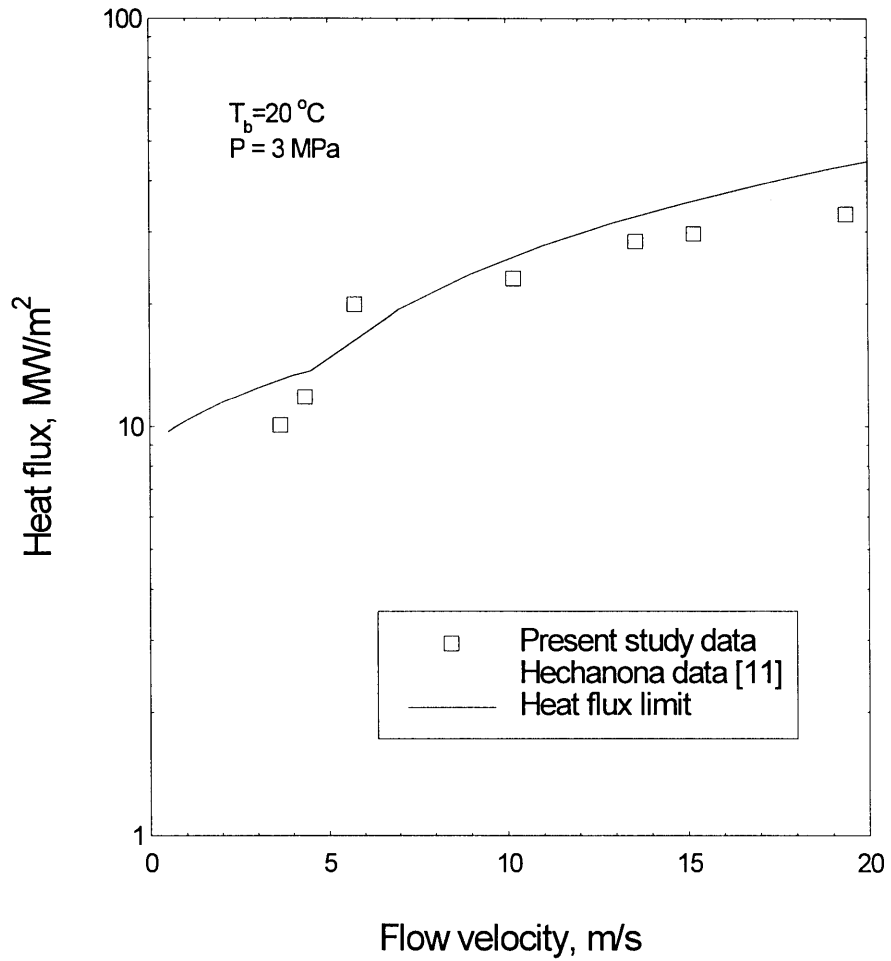AB - Unstable film boiling region

BC - Stable film boiling region

Figure 12: Heat flux limit (Equation (24)) as a function of flow velocity